AN EXPERIMENTAL STUDY OF MATERIAL TRANSFER UNDER THE INFLUENCE OF MAGNETIC FIELD

By

RAJESH INDURKHYA

DEPARTMENT OF MECHANICAL ENGINEERING

N INSTITUTE OF TECHNOLOGY KANPUR

APRIL, 1985

AN EXPERIMENTAL STUDY OF MATERIAL TRANSFER UNDER THE INFLUENCE OF MAGNETIC FIELD

A Thesis Submitted
in Partial Fulfilment of the Requirements
for the Degree of

MASTER OF TECHNOLOGY

By

RAJESH INDURKHYA

to the

DEPARTMENT OF MECHANICAL ENGINEERING

INDIAN INSTITUTE OF TECHNOLOGY KANPUR

APRIL, 1985

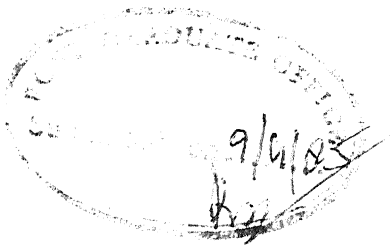

CERTIFICATE

This is to certify that the thesis entitled, "An Experimental Study of Material Transfer Under the Influence of Magnetic Field" by Rajesh Indurkhya is a record of work carried out under our supervision and has not been submitted elsewhere for a degree.

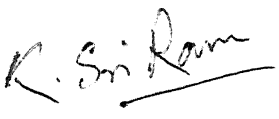

K.Shri Ram
Professor & Head
Department of Nuclear Engg.
IIT Kanpur

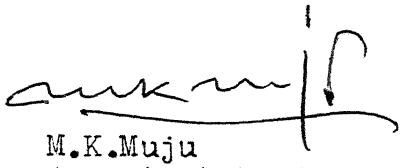

M.K.Muju
Assistant Professor
Dept. of Mech. Engg.
IIT Kanpur

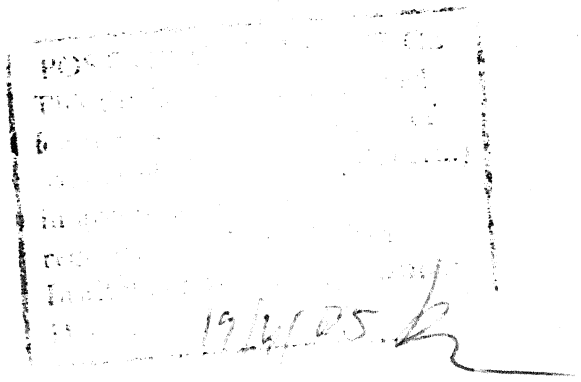

ACKNOWLEDGEMENTS

It is with immense pleasure and great respect that I express my deep sense of gratitude to Dr.K.Shri Ram and Dr.M.K.Muju for their invaluable guidance and encouragement throughout my thesis work.

I take this opportunity to express sincere thanks to all my friends for creating a congenial atmosphere and making my stay at IIT enjoyable and memorable.

Rajesh Indurkhya

CONTENTS

LIST OF FIGURES AND TABLES

LIST OF TABLES

ABSTRACT

Metal transfer under the influence of magnetic field has been studied. Mild steel block (used as workpiece) and tungston carbide ball are used as matting pair. The proton induced X-ray emission technique is used for the estimation of iron transferred to the tungston carbide ball. The longitudinal grooves are cut on the mild steel block with tungston carbide balls at different cutting speeds and under different magnetic field strengths. Thus the quantity of iron transferred on the tip of ball is estimated. It is found that the amount of metal transferred is increased in the presence of magnetic field. Its value is low at lower speed, reaches to a maximum value, with the increase in cutting speed, with the further increase of cutting speed its value decreases. It is observed that the transferred metal appears as a bright flake. At high speed the groove appears shiny. It is also found that the surface roughness is increased in the presence of magnetic field. At the same field, surface roughness decreases with the increase of speed and tends to reach a constant value. These metal transfer results show similar behaviour as obtained in adhesive wear reported by other workers.

CHAPTER 1

INTRODUCTION

1.1 INTRODUCTION

"Wear is the progressive loss of substance from the operating surface of a body occurring as a result of relative motion of surfaces". This is a very broad definition and according to this wear covers so many materials, sliding systems, operational conditions and types of measurements. It is a complex process involving interaction between various fields of science and engineering.

Because of the presence of surface irregularities on the real surfaces, contact between solids occurs only at certain asperities. A study of these contact points provides informations concerning adhesion, friction and wear process. When two asperities interact they may deform, weld and subsequently fracture to produce a loose wear fragments. This process of welding and deformation can also lead to diffusion across the interface. As the number of asperities reduces i.e. the smoothness of surface increases, the wear between sliding or mating surfaces reduces. It is natural therefore that considerable research on wear phenomenon has been done taking into consideration

various conditions of load, temperature, environment and other external parameters (physical, chemical, electrical or magnetic in nature) with the objective of improving the wear and adhesion characteristics of interacting surfaces.

Metallic wear and surface deterioration in the presence of magnetic field has been studied by a limited number of researchers [1-6]. Muju and Ghosh [4-6] have done fairly extensive investigation on wear under magnetic field. They have proposed a phenomenalogical model and have found that almost all experimental results reported are in agreement with the model and theoretical postulates. They have concluded that the magnetic field basically influences the adhesive wear characteristic of the rubbing pair and the relative magnetic permeability and hardness seems to be the predominant factor. The effect of magnetic field is seen through its influence on the mobility of dislocation. They also suggest that dislocation mobility should influence the diffusivity across the interface which can lead to different surface hardness gradient at the surface. The adhesive wear behaviour of the sliding pair

can correspondingly get changed. It therefore appears that the application of the magnetic field basically alters the wear behaviour of rubbing pair rather than wear resistance of an individual body. Also it is not always advantageous to apply magnetic field. In fact the surface deterioration in steel ball bearings in electrical machines observed by Simpson and Russel [7] where large magnetic field is present, could vary well due to the effect of magnetic field on wear. Magnetic field has also been seen to have effect on creep and fatigue [8-9].

1.2 TYPES OF METAL TRANSFER AND WEAR

Whenever two surfaces come in contact and there is a relative motion between them, the mutual transfer of matter takes place. This phenomenon occurs because of the facts that the friction force is experienced by the mating surfaces due to (a) instantaneous welds formed at the points of contact and (b) ploughing of high points of one surface with other surface. The rupture of these welds ultimately takes place because of the high stresses. Thus the mutual metal transfer takes place.

The wearing behaviour and metal transfer of a pair of mating surfaces would in general be governed by the factors like

(1) Material homogeneity

(2) Material properties

  (a) Resistance to fatigue loading

  (b) Resistance to impact and shear loading

  (c) Resistance to thermal effects like diffusion etc.

(3) Surface properties

  (a) Surface energy

  (b) Surface film behaviour

  (c) Surface residual stresses

(4) Presence of electrical and magnetic fields.

Wear has been in general classified as given below:

(1) Abrasion wear

This form of wear occurs when a rough surface or hard particles like carbides present in the softer matrix , slides on a softer surface, thus ploughing in softer surface takes place and continuous wear results. Rate of wear depends upon the number of hard particles per unit area, size, distribution and hardness of particles present in both the surfaces. The relative hardness of two surfaces may be altered during cutting as a result of strain hardening. At high speed even softer particlesmight dislodge due to high impact values.

(2) Diffusion wear

Solid state diffusion is the mechanism by which atoms diffuse from one lattice point to another thus leading to a net transfer of matter from one surface to other one in the direction of concentration gradient. But this happens only when temperature conditions are favourable for atomic movements. Thus if in the adhesion process

localized temperature increases to a considerable level interfacial diffusion can occur. The high temperature is produced only when the mating velocity is high. But it is not necessary always to have high temperature, diffusion also takes place at high stress and strain conditions during cutting.

(3) Adhesion wear

When two smooth surfaces are made in contact, the contact does not occur at all points of mating surfaces but it takes place only at the asperities of the two surfaces. Hence the load between them is distributed on these asperities, thus causing high stresses at these contact areas. This gives rise to plastic flow at the interface and the formation of junctions at these local points. Now if sliding commences under such conditions, the rupture of these junctions or welds takes place on the softer surface and thus metal is transferred to other surfaces. This is called adhesion wear. Thus adhesion, adhesive wear and metal transfer are intimately connected. The two types of welds that formed are;

(a) Pressure weld

It forms below recrystalline temperature under high local stresses.

(b) Temperature weld

It forms at high temperature due to high velocity. At high temperature the matrix of surfaces becomes softer and thus leading to formation of welds.

At low speed plastic deformation gets enough time to get finished and thus the weld gets sufficient time to form.

1.3 OBJECTIVE AND SCOPE OF PRESENT WORK

Experimental as well as theoretical investigations [10-12] clearly indicate that diffusion in metals is significantly enhanced during deformation. Results have shown [13-14] that diffusion takes place rapidly along the dislocations, at rates many orders faster than through the lattice. Since dislocations increase appreciably during deformation it is logical to believe that high values of diffusivities in dislocation core would also enhance the average bulk diffusion rate during plastic deformation. On the basis of these reasonings Muju and Ghosh have postulated that diffusivities in machining/rubbing

conditions can rise to extremely high values [15-16]. Since the magnetic field would enhance the dislocation velocity, the value of diffusivity would be further increased. This would lead to greater adhesion at the interface and under conditions of higher strain rates (machining speeds) and higher temperatures this would result in a negative hardness gradient in materials like brass rubbing against steel, a feature repeatedly observed by the authors. Considerable iron has been detected as integral part of brass flakes collected in wear studies.

Srivastava [17] has reported that even after dressing of grinding wheel by over several hundred microns the X-ray flourescence results of grinding grains indicated some residual metal after subtracting the background readings. It is believed that the residual material is actually diffused. On the basis of these evidences and reasoning, it is believed that considerable diffusion is possible in rubbing or scratching as well as machining operation. Similar results have been found by Konig [18]. But Shaw [19] has shown that although the temperature at the interface of matting surfacesis very high, often exceeding the melting temperature of the workpiece, but the time duration is very small for any metallurgical effects. Shaw suggested that there is insufficient time

for any diffusion controlled structural change to occur which may have a bearing on the loading phenomenon.

The objective of the present work was to identify experimentally diffusion of iron into tungston carbide under various rubbing speeds and magnetic fields. Due to repeated failure of the Si(Li) detector in PIXE unit the work was ultimately restricted to examination of adhesive material transfer alone. Study of diffusion would involved removal of adhered metal (iron) by etching and resubmitting the ball to PIXE to detect the diffused material. This part of work could not be taken up due to non-availability of unit because of heavy schedule.

Examination of these balls for any possible diffused iron in them would form a possible and interesting follow up of the present work. It may be emphasised that PIXE measurement technique, used in the present work, is nondestructive in nature hence the samples can be preserved and can be resubmitted to PIXE analysis at a later date for measurement of diffused iron.

CHAPTER 2

EXPERIMENTAL TECHNIQUES AND PROCEDURES

2.1 TECHNIQUES OF STUDYING METAL TRANSFER AND WEAR

Various measurement techniques have been used by the investigators for the evaluation of metal transfer. These techniques include the calorimetric method, chemical detection technique and photospectroscopic methods etc. Most of these techniques are time consuming, painstaking and destructive type and are not sufficiently accurate for the evaluation of material transfer as involved in machining processes. Subsequently different types of sensors were developed to detect the amount of metal transfer. Metal transfer has also been measured quantitatively using $\gamma - \gamma$ coincidence and extrapolation methods with irradiated workpieces having γ-emitting radiotracers of long half life. In these unconventional methods, radiation hazard due to handling of radioactive chips and contamination of machine was a serious problem.

In general the amount of metal transfer on the tool is of very small order. In case where single grain or cutting point is considered its value is very small of order in nano to micro grams. Thus the techniques which are commonly used for the estimation of trace elements

should be able to predict the amount of metal transfer accurately. The methods that are commonly used for the quantitative and qualitative estimation of trace elements are:

(1) Optical emission spectroscopy
(2) Atomic absorption spectroscopy
(3) Neutron activation analysis
(4) Electron microprobe analysis
(5) X-ray fluorescence spectroscopy
(6) Auger electron spectroscopy
(7) Proton induced x-ray emission (PIXE).

These are discussed in short as follows:

In optical emission spectroscopy it is usually difficult to obtain uniform excitation over the entire area of the sample using an arc or spark source. Even the use of radio frequency coupled plasma may not be very suitable for quantitative estimation.

Atomic absorption spectroscopy requires the sample should be in the liquid form and the analysis of only one element is possible at a time. Also it is difficult to analyse some elements using this technique. But this technique has proved to be one of the most widely used and successful techniques for trace element analysis. It is quantitative, sensitive, simple, rapid

and relatively inexpensive. Recent development such as non-flame atomization systems, have significantly increased the analytical sensitivity of the method for many elements making it a truely micro analytical method. For all practical purposes,a separate source is needed for each element to be determined.

The neutron activation analysis is the most sensitive technique for trace elemental analysis. However, for a sample having large number of elements, spectrum is quite complex and analysis is difficult. Further, it is known that the neutron activation analysis has somewhat poor detection limit for some elements like Pb, Fe and S when compared to the detection limit obtained for many other elements. However if irradiation facilities are available, activation analysis is preferred to radiotracer elements. If the activation analysis is impossible or difficult because of self shielding or counting problems or due to overall radioactivity of the sample or nuclear reactions, radiotracer methods are found useful because of simplicity and low cost.

The electron microprobe analysis involves an electron gun with sophisticated focusing such that the electron beam strikes a very small area of the target sample. This technique is restricted to solid samples

because of the high vacuum necessary to operate the electron beam with the required degree of flux. The technique does not offer the required sensitivity because of the very small area of excitation and shallow penetration. The detection limit is usually poor due to the presence of large bremsstrahlung background.

The x-ray fluorescence technique comes under the category of energy dispersive x-ray spectroscopy analysis. This technique offers low cost, rapid, reliable and simultaneous multielemental analysis. This technique is applicable to the quantitative and qualitative estimation of the elements present in metallurgical samples, agricultural samples, biological, geological samples, the elements present in the environmental such as air, water food samples etc. In this technique no sample preparation is usually necessary. This is a great advantage for aerosol studies. The material collected on the filter paper may be used directly. The advantage is that the samples are not destroyed during the analysis so that they may be preserved for future use.

Auger electron spectroscopy can be used to analyse layers of few atoms thickness both qualitatively and quantitatively. In this techniques the successive layers can be removed from the surface by sputter etching

and simultaneously the elements can be traced. This process involves bombardment of the surface with a stream of argon irons to etch the specimen surface through removal of surface layers. It is important that the area subject to sputter etching be much larger than the area of the electron beam so that the region of analysis is in the centre of a relatively flat bottomed crater. The diameter of the ion beam is of the order of a few millimeters, while the electron beam can be focussed down to 25 μm. After each short etching operation the surface can be again analysed. In this way the variation of chemical composition from the surface into the interior can be determined.

Proton Induxed X-ray Emission (PIXE) also comes under energy dispersive x-ray spectroscopy technique. This technique is more sensitive than any other technique. It can detect the elements in parts per 10^6 - 10^7. It analysesthe very small absolute amount of sample as low as 10^{-12} gm with full sensitivity. It is also non-destructive in nature. This technique is used in the present work. The details of this technique are discussed in the next section.

2.2 PIXE AS A TOOL FOR WEAR AND METAL DETECTION STUDIES

As the amount of metal transferred from work-piece (annealed mild steel) to the tungston carbide ball (tool) is very small and of the order of nano to micro grams, it can not be measured very accurately by the conventional techniques available. Proton Induxed X-rays Emission technique has therefore been used. This technique in fact traces all the elements present in the sample. A little introduction about the technique is given below.

In most of the nuclear technique the fundamental particles are used for the basic research. These particles are accelerated at very high velocities and when these accelerated particles say protons are allowed to bombared or strike on a target, several nuclear (typical), phenomenon such as, emission of gamma rays, photons, leptons, nucleons etc. take place as shown in Fig.(1). These phenomenon posses information about different aspects of structure and properties of nuclei. Not only these but purely nuclear effects, important atomic processes also occur simultaneously. The protons interact with the atomic electrons of the target material either ejecting or exciting them. These give rise to x-radiations characteristics of the elemental composition of the target.

It was first shown by Johansson [20] that a combination of x-ray excitation by protons and detection by a silicon detector constitutes a powerful multi-elemental analytic method. The important features of this method are —

(i) Multielemental nature so that in one exposure all constituent elements can be identified and estimated.

(ii) High sensitivity and accuracy

(iii) Very small absolute amount of sample, as low as 10^{-12} gms can be analyzed with full sensitivity.

(iv) Non destructive nature.

2.2.1 Production of X-rays

X-rays are produced under proton bombardment of atoms. The atomic energy levels are quantized. In fact these energy levels are manifestations of electronic excitations. The energy states are characterized by a set of quantum number. The expression for electronic energy depends primarily on the principal quantum number.

When the incoming proton beam strikes the atom, ransfers part of its energy to any shell (say K shell tron) and knocks it out. The vacancy thus created

can be filled with an electron from one of the outer shells subject to quantum-mechanical selection rules. If the vacancy is filled by an electron from the L shell, then K_α x-ray will be emitted in this transition. The selection rules basically involve the changes in quantum number in a transition.

The inner shell ionization in proton-atom collisions is mainly responsible for the production of proton induced x-rays.

2.2.2 Experimental Method

(A) Basic Set up

Firstly the proton beam is generated and accelerated by the 2MV Van de Graaff accelerator. It is then focussed by quadrapoles. After this it is allowed to pass through a system of collimators and is finally allowed to incident on a target mounted at the centre of a specially designed scattering chamber. The x-rays coming from the target in the scattering chamber are received by a Si (Li) detector. Signals from this detector are further received by a multichannel analyser. Finally the printer is connected to the multichannel analyser and the output (counts) is printed on it. The line diagram is shown in Fig. (2).

(a) Scattering Chamber

The target chamber is made of brass and in cylindrical shape. There is an arrangement to couple this with a silicon lithium detector in standard liquid - nitrogen cooled cryostat with or without a separation window. A 10 micron thick mylar window separates the detector from the chamber. The sectioned view of chamber is shown in Fig.(3).

(b) Detector

The ORTEC detector with energy resolution of 160 eV at 5.9 KeV has been used.

(B) Target Preparation

Preparation of suitable targets is of prime importance in PIXE analysis. In most cases the use of thin targets (few hundred $\mu g/cm^2$) is preferred so that the proton energy loss in the target and absorption of emitted x-rays in matrix can be neglected in case of heavy elements. For light elements (Atomic Number $Z \lesssim 20$), the "Second correction" is important and can be evaluated approximately if the target thickness is uniform and is known. For quantitative analysis uniformity of thickness and homogeneity of the composition are important.

The simplest case is the direct bombardment of the sample without any backing material, for instance the case of biological tissues. Mostly it is not possible to produce a self supporting target satisfying the requirements hence targets are usually supported by some suitable backings. The backing must be (i) thin, (ii) having low atomic number $Z \leq 13$ and minimum high Z impurities, (iii) having sufficient mechanical strength to withstand irradiations and manual handling.

Laboratory made formvar films are most suitable backing. Such backings satisfy most of the criterion listed above except that it has small amount of Fe impurity. The extent of this interfering element need to be evaluated before the film is used as backing.

Aluminium is also used as backing material because of its low atomic number. In the present case the tungston carbide ball is held between two aluminium sheets, having small holes at their centres so that ball can project well outside. As the aluminium sheets have lot of iron impurity hence the projected portion of the tungston carbide ball was shielded by a 100% pure aluminium foil of sufficient thickness. A small hole (dia 3.30 mm) is drilled at the centre of the foil so that cutting portion of the ball on which the metal is stuck during cutting

can be projected and can be bombarded by the proton beam. As in the target chamber we can mount 4 samples at a time hence such 4 mountings were prepared. The mounting is shown in Fig. (4).

(C) Principle

The basic idea is to provide a restricted beam so that the protons strike the target alone and the corresponding x-rays alone are detected by the Si (Li) detector. At least one of the following condition should be satisfied in quantitative analysis of the PIXE method.

(1) The target should be of uniform thickness and homogeneous in nature.

(2) The proton beam should be of uniform intensity.

(3) The target thickness profile and beam intensity profile should be known.

If the first condition is satisfied, then the beam could be of any size smaller than target. In this case beam can be focussed directly on the target by removing the Ni Foil from the beam path. In this case three collimators are used, the first one is used to clean the "halo" (6.5 mm dia), the second one to define the beam (5.0 mm dia) and the third one (6.5 mm dia) to

remove scattered protons from the defining slit.

But it is not easy always to prepare uniform targets and depending upon the method of preparation the target thickness profile is also variable. In such a case (the most common case) the beam spot must be larger than the target and the second criterion must be satisfied.

The third criterion is most difficult as target thickness profile is not easily measurable.

In order to have a homogeneous beam protons are allowed to pass through a diffuser foil (Ni) before striking the target as shown in Fig.(6).

Collimators are located inside the collimator tube in order to define the diameter of beam. The intensity profile is measured by one mm^2 (1x1) nickel foil as probe.

The beam diameter should be only slightly larger than sample size since otherwise unnecessary background radiations would be observed from backing. This larger beam spot also permits a small variation of location of the target, although case was taken to place it right at the centre of the backing.

(D) Procedure, Data and its Processing

The target is mounted in such a way so that the incoming proton beam strikes it at 45° as shown in Fig.(6). The x-ray detector is placed at 90° to the incident beam. This arrangement allows the detector to be moved very close to the target so that a larger solid angle can be utilized.

The incident x-rays transfer energy to the silicon K electrons but may not always deposit the full energy in the detector. Sometimes, a part of the kinetic energy of the K electron is lost when it escapes from the surface of the detector, and because of these events we get low energy trails to the characteristic x-ray peaks in the spectrum. It is also possible that a silicon K_α x-ray escapes without detection if it is produced near the surface of the detector. These events would give rise to spurious peaks (1.74 KeV) below the true peaks, and creating undesirable confusion. Hence to avoid these disturbing effects we use a collimator in front of the detector so that the x-rays do not interact near the edges of the detector.

The pulse from the preamplifier is fed into an amplifier and then to a Multichannel Analyzer. The output from the multichannel analyzer is printed by a

printer. The pulses are called counts. And for one sample approximately by 1/2-1 hr, we collect the counts. After knowing this the counts are plotted against the channel number. Now in order to identify the elements corresponding to the x-ray peaks, one needs the energy - channel number calibration. Thus knowing energy level at every channel number one gets the energy level at these channel number those corresponds to peaks. Also from the table of element showing their energy levels, the identification of elements is done. Thus, all the elements can be traced, in this manner.

2.3 EXPERIMENTAL SET UP

(a) Rubbing Experiment Set up

All the rubbing tests were conducted on the horizontal milling machine. An aluminium disc of 20 cm dia and 2.54 cm thickness was mounted on the arbor of milling machine. A tungston carbide ball of dia 4.35 mm was fixed on the periphery of disc as shown in Fig.(7). This type of mounting of ball is similar to overcut fly milling operation. There are also two other mounting methods one is (i) plain fly milling, (ii) face fly milling. But both these have their disadvantages of

experiencing large dynamic shock load during operation.

An annealed (950°C, time 24 hr cooling time) mild steel block of 8x8 cm cross section and 20 cm length was used as workpiece. All surfaces of the block were ground on the surface grinder. Then it was mounted on the table of milling machine. The top face of the workpiece was well polished and made parallel to bottom surface, on which grooves were cut.

A solenoid was used to magnetise the mild steel block. In fact the mild steel block acted as the core of solenoid. D.C. supply of different magnitudes of current was used. The set up is shown in Fig.(7). A dial indicater of 0.001 mm least count was used to give depth of cut - to give more accurate depth setting than possible with the milling machine table (in the present case depth of cut is taken 0.03 mm).

For each speed with or without magnetic field fresh tungston carbide ball was used. Before using them all balls were washed with acetone to remove any grease or surface layers which could affect rubbing or machining.

(b) PIXE Experimental Setup

After performing the rubbing experiments the proton induced x-ray emission technique is used for the measurement of the metal transferred on the tungston

carbide balls.

A special mounting was made to load the ball inside the testing chamber of PIXE unit. As discussed in article 2.2.2 (B) under preparation of target, that backing material should have $Z \leq 13$. In this work, commercial aluminium sheet was used as backing. Two rectangular pieces of aluminium sheet were drilled, a clear hole at their centres and the ball was pressed between the pieces and pieces were screwed. Thus the tip of the ball on which metal gets stuck, is now projecting outside. Since the commercial aluminium contains lot of iron as the impurity it was very necessary to shield the some of the area of aluminium mounting which may otherwise be hit by proton beam. A nearly 100% pure aluminium foil of 10 mm dia was used for sheilding. A hole of 3.30 mm dia was drilled at the centre of the foil so that the adhered metal on the ball can very well expose to the incoming proton beam, the mounting is shown in Fig.(4). Since 4 samples can be mounted at a time in detecting chamber so 4 identical mountings were made .

2.4 EXPERIMENTAL PROCEDURE

A number of tests were performed on the milling machine at different speeds and at different magnetic fields. The pattern of grooves cut on mild steel block is shown in Fig.(5).

These test samples (tungston carbide balls) were mounted in aluminum mountings and then loaded inside the detecting chamber of the PIXE unit. Each mounting was numbered so as to avoid the mixing of samples. Each test sample was run for 1/2 to 1 hour and the counts/channel were recorded by multichannel analyser. On plotting these counts against channel numbers the spectrum of the elements present in the sample can be seen.

After this the surface roughness (R_a value in μm) of the grooves cut at different cutting speeds and at different magnetic fields are measured by Talysurf instrument.

Roughness average R_a is defined as the arithmetic average of the departures of the profile above and below the reference line (centre line) throughout the prescribed sampling length. A little description about the method is as below.

Firstly the groove is made parallel to the traversed path of the pick up. The pick up is driven slowly across the surface and a sharply pointed stylus follows the profile of the surface irregularities. The pick up has an optical transducer and the vertical movements of the stylus are sensed photo-electrically. The signal is processed on the R_a meter. Primary necessicity is that the surface must be sufficiently levelled. For the chosen cut off (in the present case 2.5 mm) the sampling length (18.5 mm) is levelled by first touching the stylus at the beginning of groove and than it is moved forward manually, simultaneously the levelling knob is rotated so that the pen on chart should remain on the centre line upto the end of the sampling length. Now stylus is moved backward manually and again levelling knob is rotated to keep the pen on the centre of chart. This is repeated until the pen returns to the centre line of chart paper at both ends the traverse. The vertical magnification V_v is chosen (in present case 2000) such that the meter pointer should not cross the maximum limit of the meter. Thus the R_a value for all the grooves is measured. The Table 6 shows the surface roughness (R_a value in μm) of grooves at various speeds in the presence and absence of magnetic fields.

CHAPTER 3

EXPERIMENTAL RESULTS AND CALCULATIONS

3.1 CALCULATIONS

A plot ~~is~~ Shows spectrum between counts at y axis and channel number at x axis is plotted. Fig.(8), (9) and (10) shows the spectrum for fresh ball, at 100 RPM (69 m/min) without field and 100 RPM with magnetic field respectively.

The areas under the iron peak and tungston (L only) are calculated as follows:

$$A_{Fe} = \sum_{C_o}^{C_n} N_{c_i} - (C_n - C_o)\left(\frac{N_{c_o} + N_{c_n}}{2}\right) \qquad (1)$$

where, A_{Fe} = area under iron peak

C_o = channel number from where iron peak starts

C_n = channel number from where iron peak ends

N_{c_i} = iron counts at channel number C_i where $C_o < C_i < C_o$

Similarly the area under tungston peak is calculated.

As the charge intensity of the beam was kept different for some of of the samples. So it is necessary

to normalise the values of area calculated for iron peaks and tungston peaks at same charge (10 μcoul) using simple linear algebra. The normalised values are shown in Table 1 columns (5) and (6).

As all the values in Table 1, column (5) include the iron back ground present in the tungston carbide ball, so a fresh unused ball was tested and the iron area and the tungston area was calculated. It was assumed that all balls are of same composition. Now the iron area present in fresh ball was subtracted from the values of iron area for all sample after normalising it with tungston area corresponding to fresh ball. As an example for sample 1.

Iron area in sample 1 = 12255

Tungston area in sample 1 = 368117

Iron area in fresh ball (sample 9) = 3455

Tungston area in fresh ball (sample 9) = 366552

Now,

For 336552 of tungston area back ground iron area is 3455. Therefore, for 368117 of tungston area iron area back ground will be

$$\frac{3455}{336552} \times 368117 = 3779.$$

So the actual iron area for sample 1 will be 12255-3779=8776. Similarly for other samples the back ground iron is calculated and it is subtracted, thus the actual area is noted. In Table (2) column (2) is subtracted from column (3). The column (4) shows the actual iron area.

As at the last stage of measurement the unit became out of order, so calibration was not done. So the relative results were calculated. Now let λ be defined as follows:

$$\lambda = \frac{A_{Fe}}{A_W} = \frac{\text{Area of Iron (transferred to WC ball)}}{\text{Area of tungston (in WC ball itself)}}$$

The values of λ for different samples are shown in Table 3 in column 3. Table 4 shows the values of λ at different speeds and different magnetic fields i.e. amperes.

One more factor called Fe/W ratio (G) was defined as below:

$$G = \frac{\lambda_H}{\lambda_o}$$

where,

H = stands for the presence of magnetic field

o = stands for the absence of magnetic field.

The values of G at different speeds and different amperes are shown in Table 5. In wear tests G would represent a ratio of wear in presence and absence of magnetic field as used by earlier workers [4-6].

3.2 EXPERIMENTAL RESULTS

All the results are shown in Tables (4) and (5). Finally λ is plotted against cutting speed Vs. and G is also plotted against cutting speed Vs. The curves are shown in Figs.(11) and (12).

The variation of surface roughness of grooves cut (R_a value) with cutting speeds (in the presence and absence of magnetic field) is shown in Fig.(13).

CHAPTER 4

DISCUSSION AND CONCLUSIONS

4.1 DISCUSSION

The results obtained for the metal transfer during scratching of mild steel by spherical tungston carbide ball indentor at various speeds have been shown in Fig.(11). The figure shows the variation of iron per unit tungston transferred to the tungston carbide ball (λ) with cutting speeds in the absence and presence of magnetic field. The curve shows that the metal transfer first increases, reaches a maximum and finally decreases. This nature of metal transfer or adhered metal with cutting speed is very much similar to that in rubbing or scratching or sliding between two bodies [21-23]. The most possible physical explanation of this nature is as follows.

This behaviour of metal transfer is mainly due to variations in temperature and pressure at the interface of the matting surfaces at different cutting speeds. At low speed, the rise in interface temperature is very small, therefore the probability of forming welds between transferred metal and ball material is less, and hence the metal transferred is not adhered very strongly to the ball. Now when the ball will come in contact (for cutting)

with workpiece again, some of adhered metal will plucked off due to weak bond. This ultimately results in less metal transferred at low speeds.

As the cutting speed increases the temperature also increases and therefore probability of forming welds between transferred metal and ball material is more and hence it means that more metal is adhered to the ball. Apparently in the lower speed ranges the conditions of pressure and temperature are so prevalent that welding of the indentor or scriber and the surface layer of the mild steel is possible. At a critical speed the conditions are so optimum that maximum metal transfer occurs across these welds. K.I. Molanin [24] have also observed the similar metal transfer and have seen that the transferred metal is in the form of flattened bright flake. In the present work also such bright and flattened flake sticking to tungston carbide balls have been observed. These flakes are very hard and the normal work harding phenomena cannot explain this.

But if the process deeply studies, it can be argued that in the type of experiments conducted (which is similar to grinding, scratching, sliding and possibly followed by extrusion) the material layer undergoes considerably large strain similar to that in metal cutting

and at high strain rates which could enhance the strength of the adhered layer. The mechanism is shown in Fig.(14). This bright flake acts as an abrasive grain in successive cuts and it has lamellar structure. Now as the number of scratches (contacts) increases the height of adhered layer also increases i.e. quantity of metal transfer also increases, when this height reaches to a maximum value, all the excess layer of metal is plucked off in the form of chip but the amount transferred remains almost constant at a particular speed.

As the cutting speed further increases the temperature also increases and therefore such thermal conditions are developed that the hardness of the metal transferred reduced significantly and due to which the amount of metal transferred reduces considerably. It is felt that as the speed further increases the amount of metal transfer would further decrease and finally the adhered metal will completely disappear. The machined surface appears shiny (as at 87 m/min cutting speed in the present case). It shows that at low speed the surface roughness should be relatively larger than that at higher speed. It means that as the cutting speed increases the surface roughness decreases. The variation of surface roughness (R_a value in μm) with cutting speed is shown in Fig.(13). It shows

that surface roughness indeed decreases as cutting speed increases, thus giving support to the above argument.

Now as the magnetic field is applied the curve in Fig.(11) shows that it enhances the metal transfer on to the ball. The possible physical explanation of this may be that the probability of plucking off of the adhered metal will be less in magnetic field as compared to without field. The reason for this may be that now the workpiece is magnetised so(1) chips removed are also magnetised; (2) the adhered metal to ball is also magnetised and (3) it is possible that due to high stress, strain and strain rates some of iron may be even diffused inside the tungston carbide ball.

So due to magnetic force of attraction between the molecules of adhered layer, it will not plucked off as easily as possible in without field. Hence metal transfer is more under magnetic field as compared to nonmagnetic case. Fig.(13) shows that in the presence of external magnetic field the surface roughness is increased. It verifies that due to presence of magnetic field the amount transferred from mild steel to tungston carbide ball increases because of less probability of plucking off of metal adhered to the ball.

The theoretical explanation of the enhancement of metal transfer due to an external magnetic field is that when very strong magnetic field is applied to a ferromagnetic body, the internal stress reduces due to magnetostrictive stress relaxation. This causes considerable increase in mobility of dislocations. At room temperature for iron the dislocation velocity (and therefore strain rates) increases four times in the presence of magnetic field. In two mating surface the contact occurs only at the asperities. Under relative velocity and pressure these asperities get deformed and welded. The time required to reach a specific value of dislocation density in ferromagnetic body reduces considerably due to increase in dislocation velocity whereas it is not affected in nonmagnetic body. Therefore the probability of failure of function on the ferromagnetic body side is more than nonmagnetic side. Thus for a definite time the junction failure on the side of ferromagnetic body is greater in the presence of magnetic field. It means wear rate of ferromagnetic body is greater in the presence of magnetic field. Therefore in the present case the wear of mild steel is more in the presence of magnetic field hence more metal is transferred to the nonmagnetic tungston carbide ball. The experimental results obtained support the forgoing conclusions.

The values of σ, which is ratio of iron transferred in magnetic field to that in without field (λ_H / λ_o), also varies in the same manner as λ varies. The curves are shown in Fig.(12).

4.2 CONCLUSIONS

(1) The external magnetic field enhances the metal transfer during the process of cutting or scratching or rubbing.

(2) The metal transfer increases with cutting speed, reaches a maximum and then decreases with further increase of speed.

The variation of σ factor (λ_H/λ_o) with rubbing speed is quite similar to that observed in rubbing (and cutting) of mild steel with brass/H.S.S. as shown in Fig.(15). Thus it can be concluded that there is close similarity in the influence of magnetic field in cutting, rubbing and scratching.

(3) The surface roughness of the surface machined increases in the presence of an external magnetic field for a particular speed. However, under the same field the surface roughness decreases with the increase of speed and tends to reach a constant value.

The physical examination of groove indicates a periodic removal of layer in mild steel block leading to higher surface roughness under magnetic field. It is also possible that friction may also be higher with magnetic case, a feature also observed by an earlier worker [25].

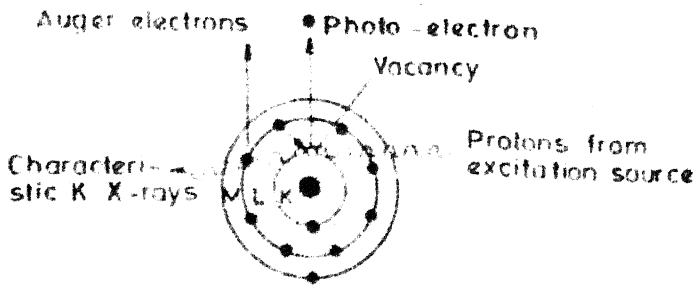

FIG. 1 SCHEMATIC DIAGRAM SHOWING THE GENERATION OF CHARACTERISTIC K X-RAYS FROM SODIUM ATOM

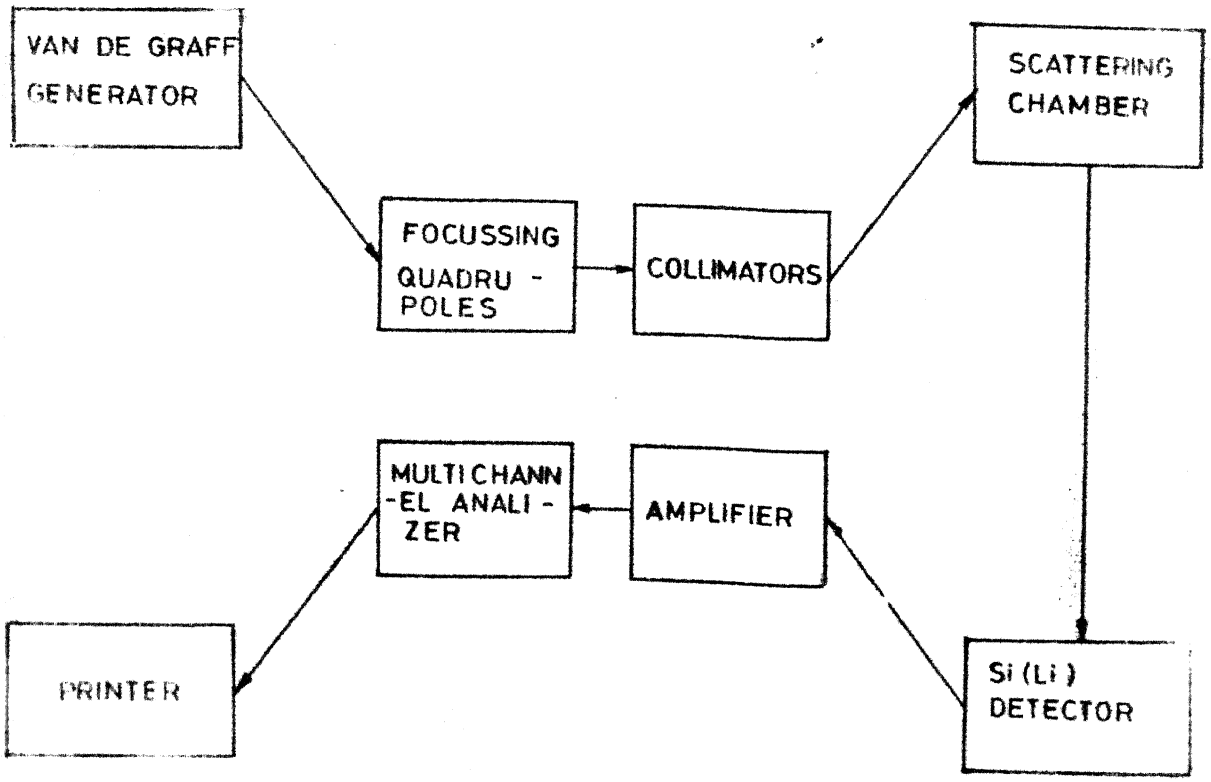

FIG 2. LINE DIAGRAM OF PIXE UNIT

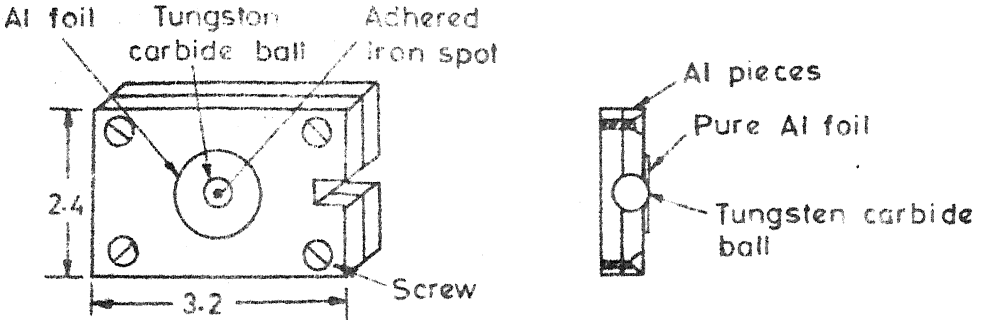

FIG. 4 Al MOUNTING FOR PIXE MEASUREMENT

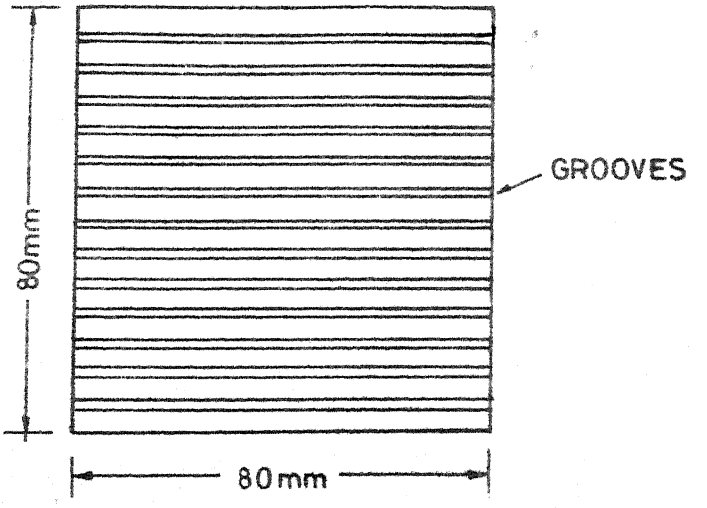

FIG 5 GROOVES CUT AT VARIOUS SPEEDS AT UNDER DIFFERENT MAGNETIC FIELDS

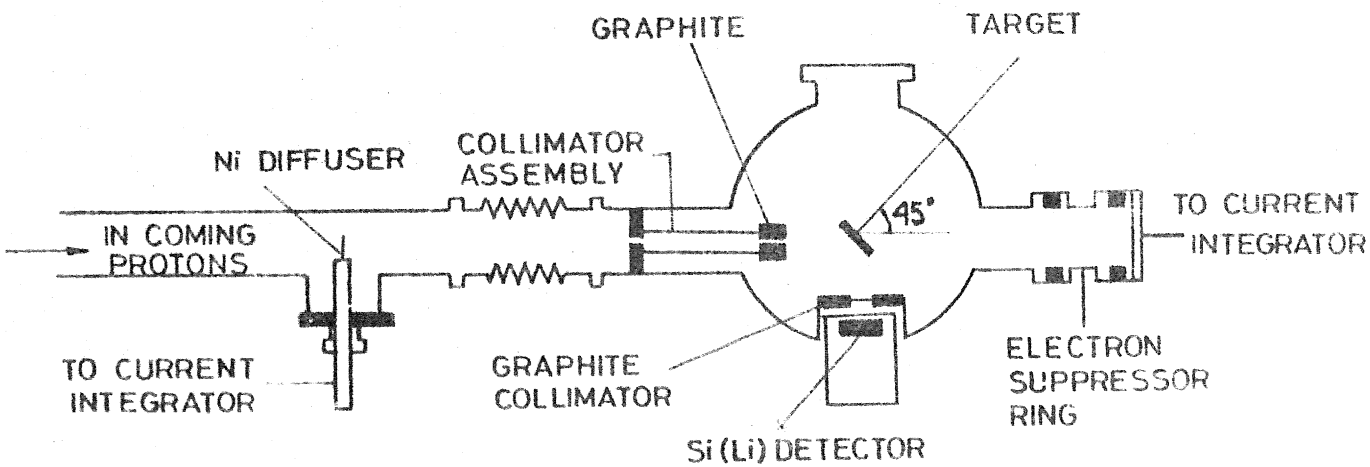

FIG 6 SCHEMATIC ARRANGEMENT OF PIXE UNIT

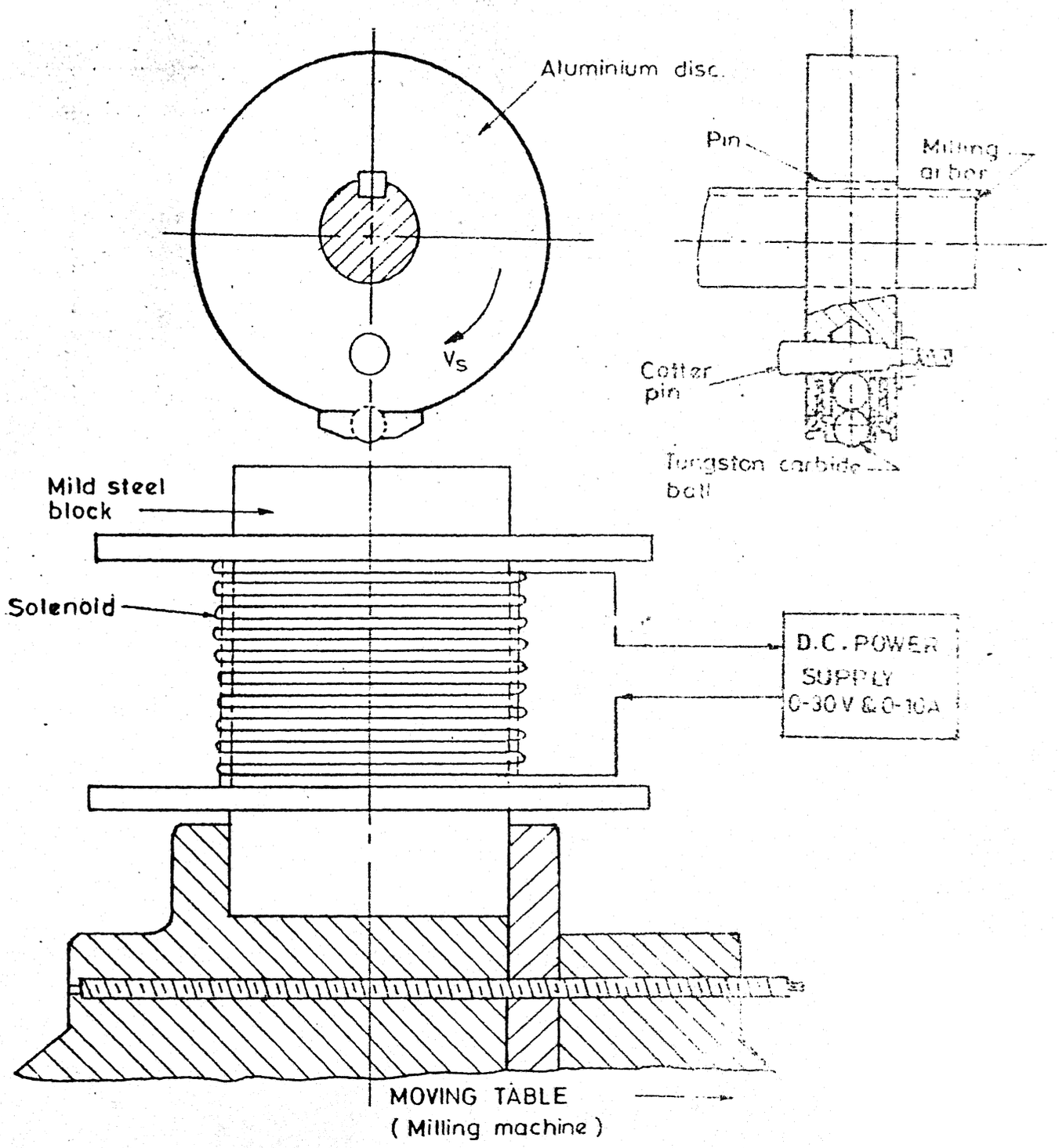

FIG. 7 EXPERIMENTAL SET UP

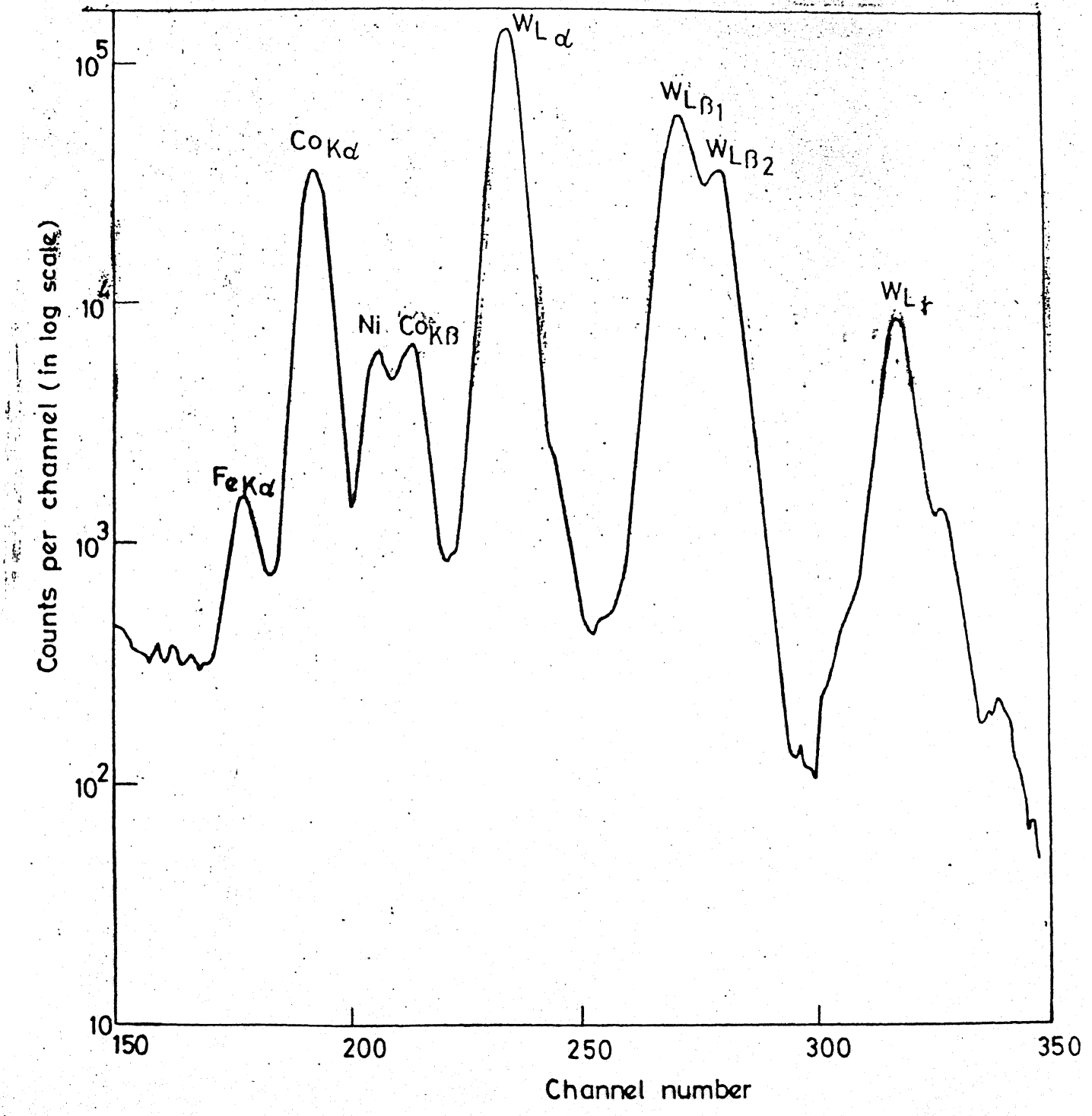

FIG. 8 SPECTRUM SHOWING THE ELEMENTS IN FRESH UNUSED TUNGSTON CARBIDE BALL

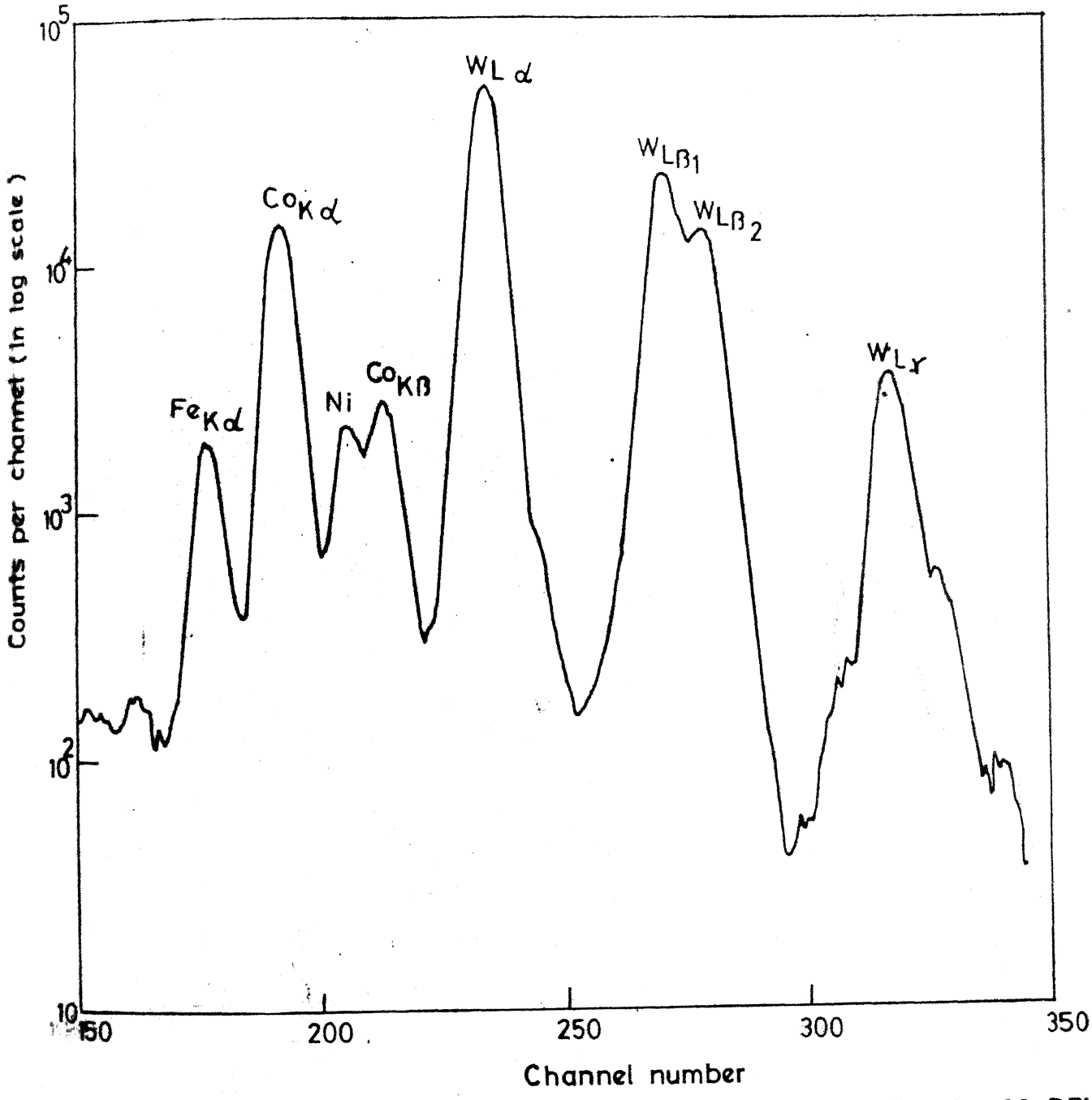

FIG. 9 SPECTRUM SHOWING THE ELEMENTS FOR THE SAMPLE AT 100 RPM WITHOUT MAGNETIC FIELD

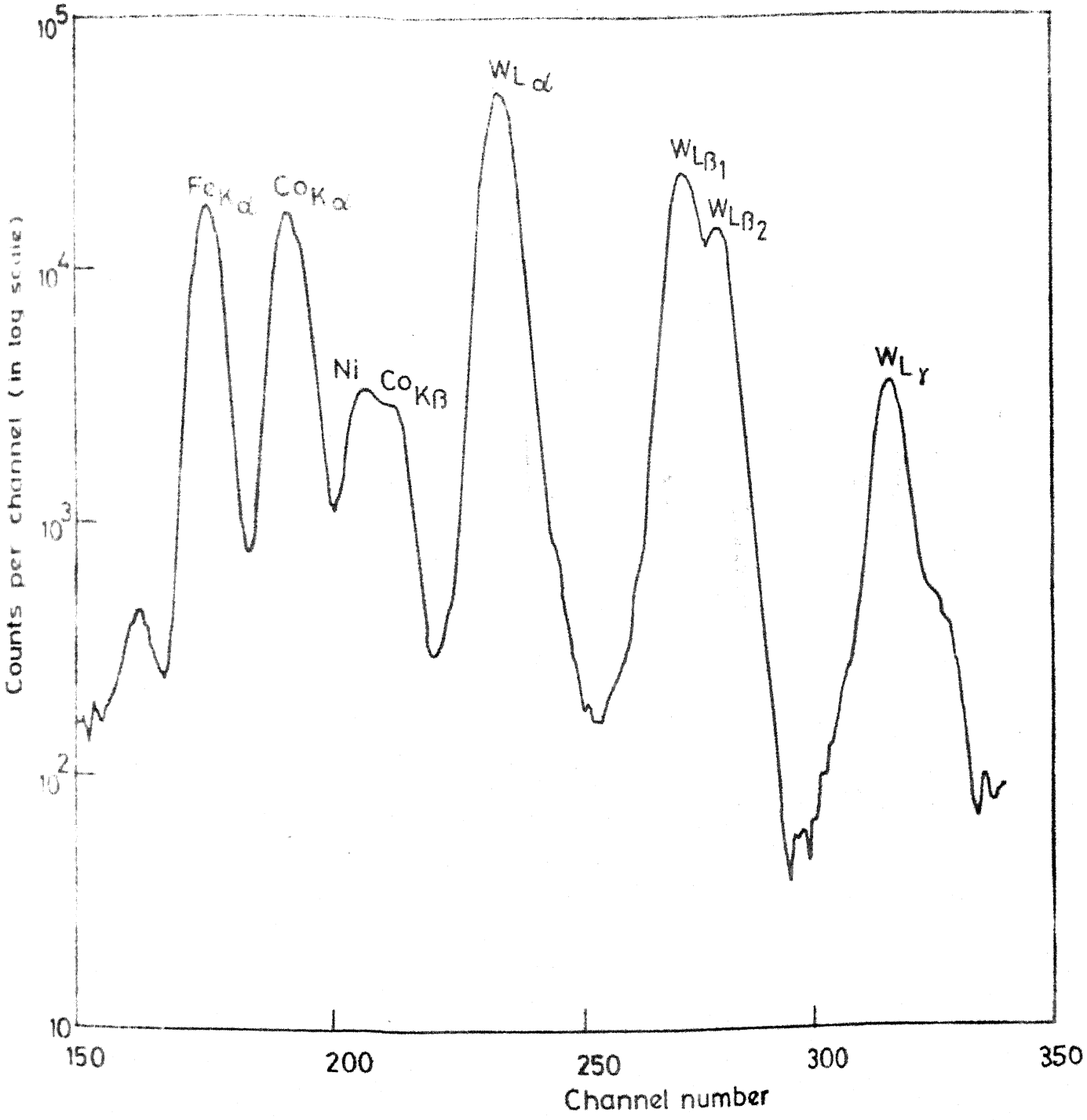

FIG 10 SPECTRUM SHOWING THE ELEMENTS FOR THE SAMPLE AT 100 RPM WITH MAGNETIC FIELD

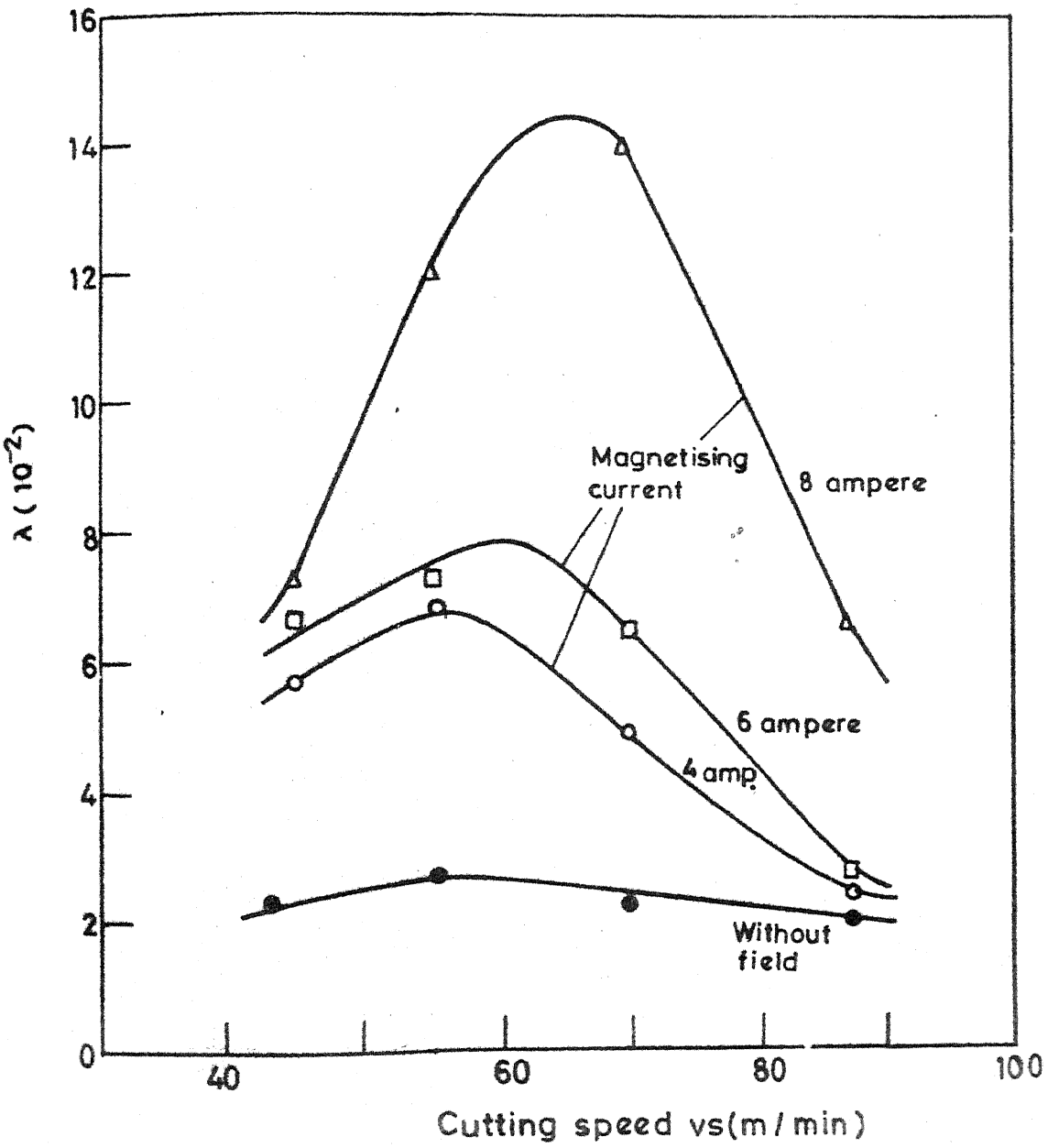

FIG. 11 VARRIATION OF RATIO OF IRON TO TUNGSTON (λ) WITH CUTTING SPEED

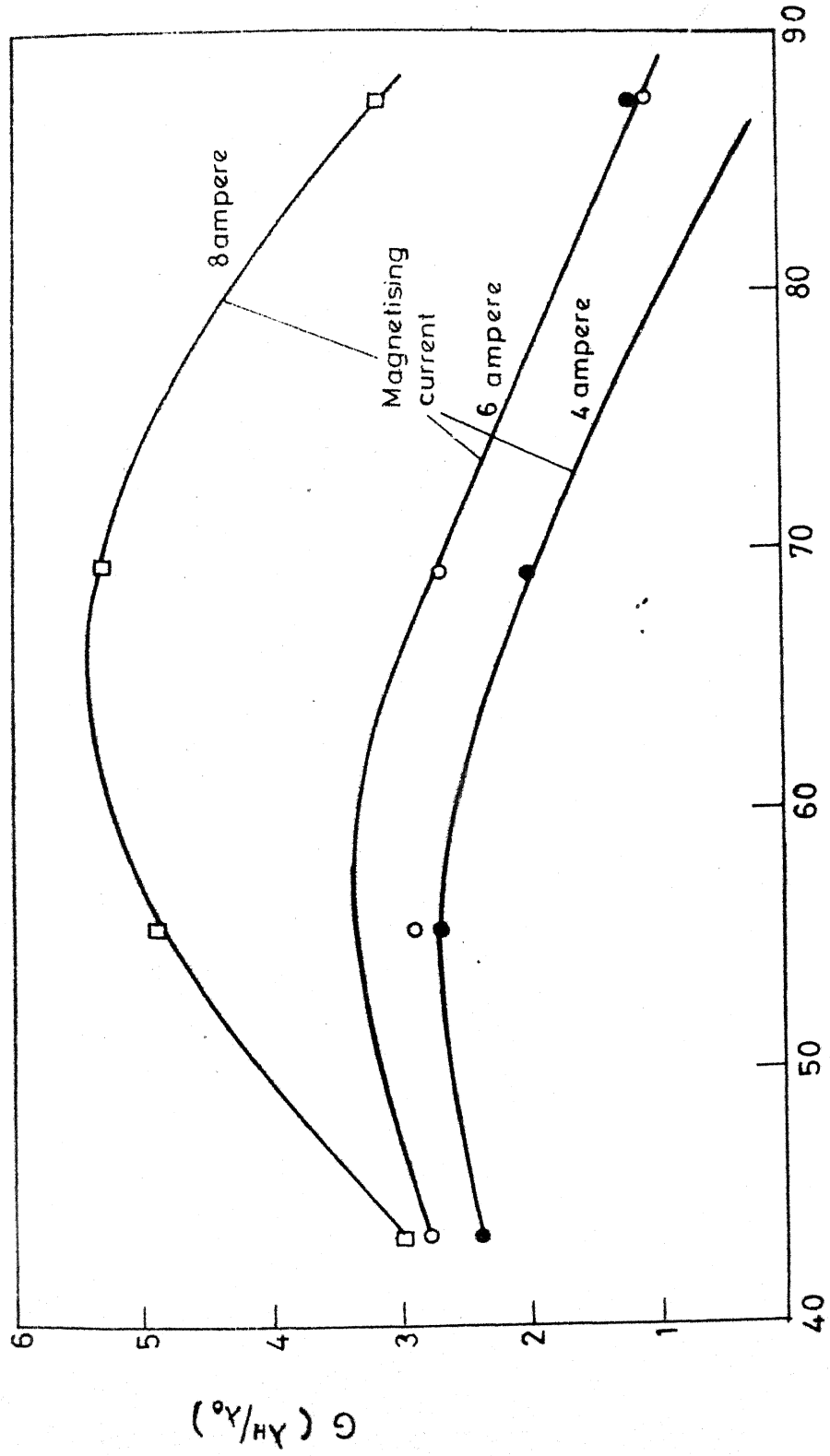

FIG. 12. VARIATION OF Fe/W RATIO (G) WITH CUTTING SPEED

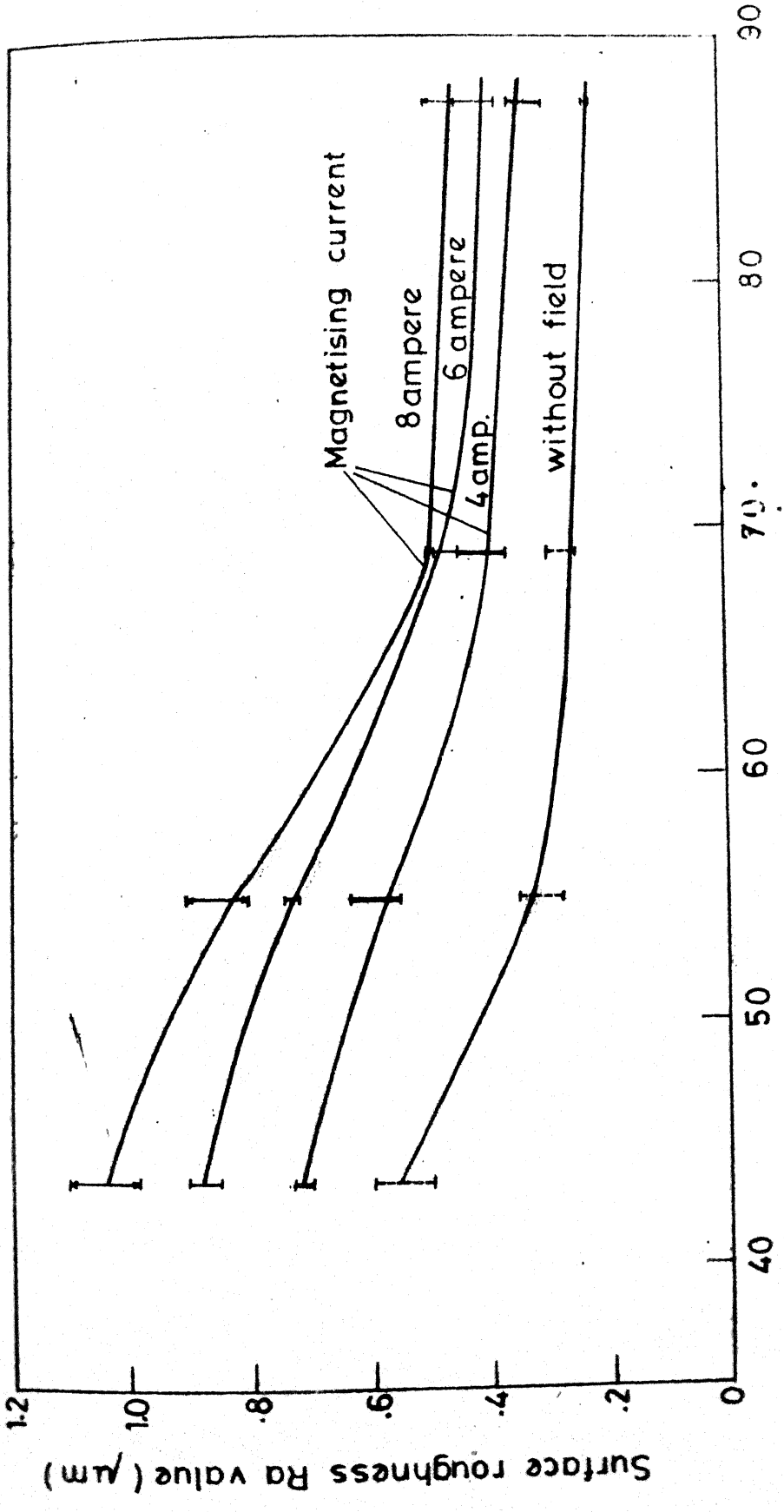

FIG 13. VARIATION OE SURFACE ROUGHNESS (Ra value in µm) WITH CUTTING SPEEDS AT DIEFERENT MAGNETIC FIELDS

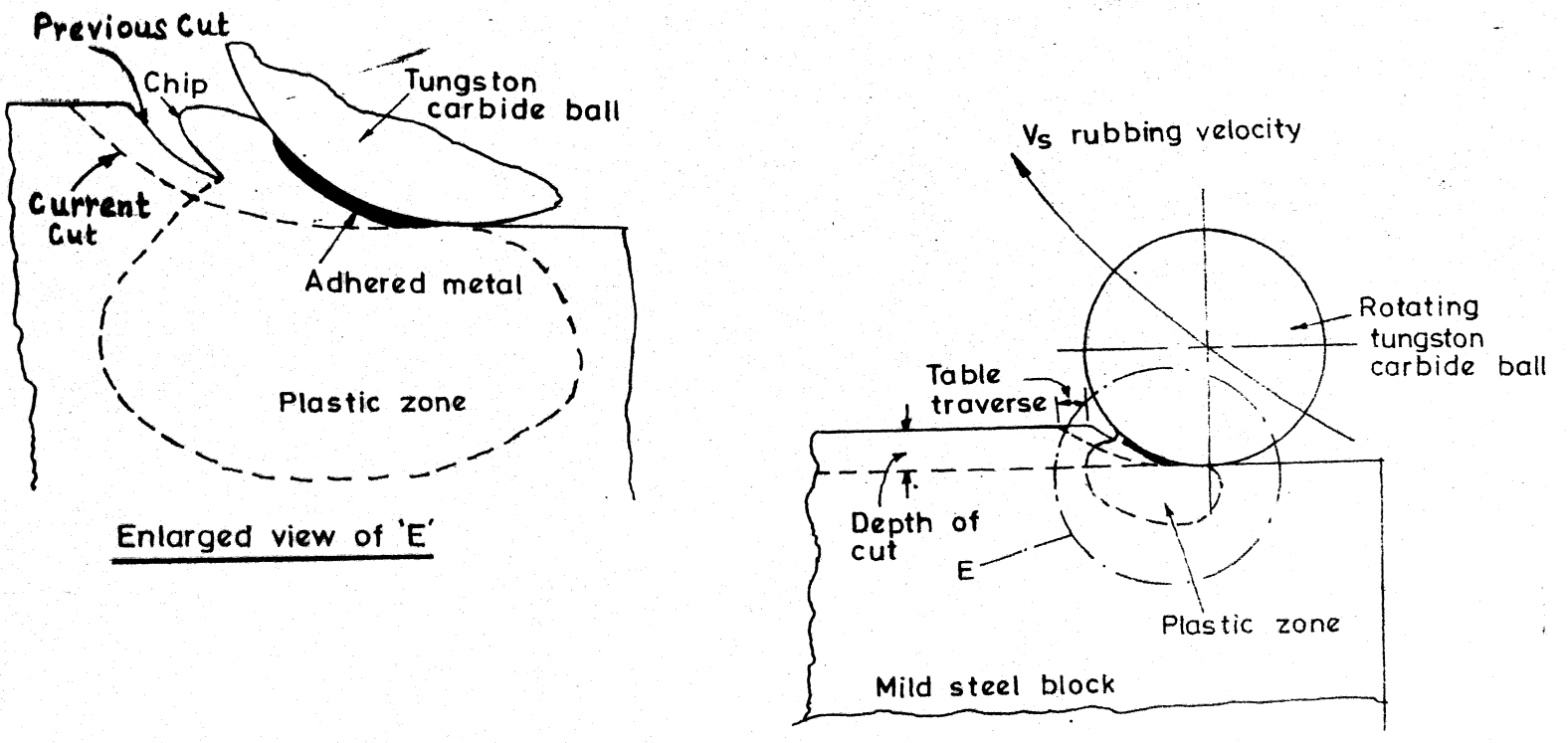

FIG. 14. MECHANISM OF METAL ADHESION ON T.C. BALL AND REMOVAL FROM MILD STEEL BLOCK

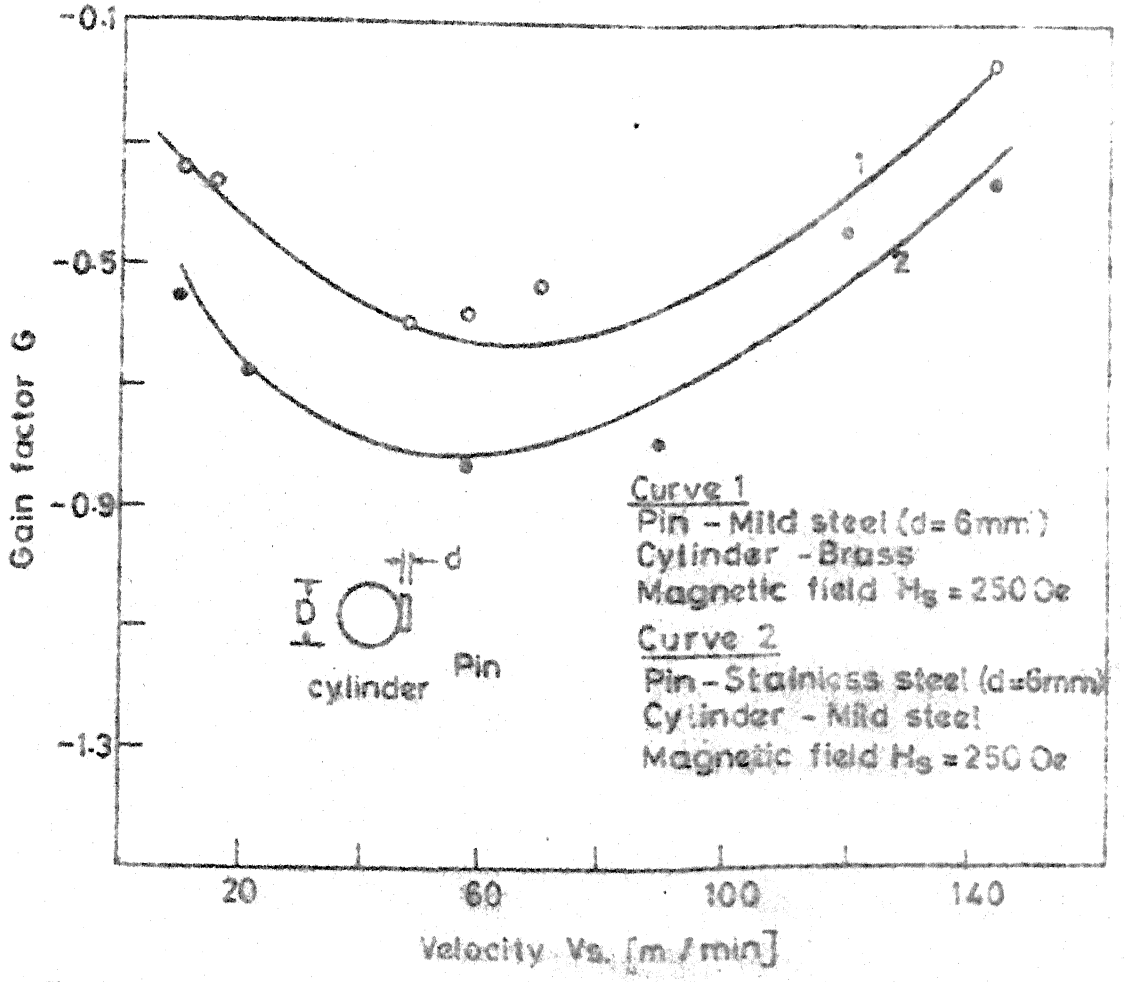

FIG. 15 VARIATION OF GAIN FACTOR WITH RUBBING VELOCITY
(Ref. [4])

SPECIFICATIONS OF EXPERIMENT

1. Tungston carbide ball dia = 6.35 mm
2. Dia of aluminum disc = 20 cm
3. Effective radius of rotating ball = 107.28 mm
4. RPM of wheel at which readings are taken = 63 (43.5 m/min), 80 (55.25 m/min), 100 (69 m/min), 125 (87.35 m/min)
5. Depth of cut = 0.03 mm
6. Milling table speed (ie workpiece) = 10 mm/min
7. Cross section of mild steel block = 80x80 mm
8. Length of mild steel block = 20 cm
9. Length of solenoid = 7.8 cm
10. Number of turns = 725
11. Magnetising current range = 0, 4, 6 and 8 ampere
12. Material hardness (Mild steel workpiece) = 98 RH_B

Table 1 : Normalised values of Iron & Tungston Peak Areas

Sample No.	Beam charge in M coul	Area under Iron Peak	Area under Tungston peak	Normalised Iron Peak for 10 coul	Normalised Tungston Peak for 10 coul	
(1)	(2)	(3)	(4)	(5)	(6)	
1	10	12255	368117	12255	368117	
2	20	42212	559540.5	21106	279770.25	
3	20	35630	643402	17815	321701	
4	10	33529	403396	33529	403396	
5	20	29627	366826	14813.5	433413	
6	10	26918	345960	26918	345960	
7	20	18518	590844	9259	295422	
8	10	17155	455528	17155	455528	
9	30	10365	1009656	3455	336552	Fresh Ball
10	20	38341	640985	19170	320492	
11	10	23445	296290	23445	296209	
12	10	27411	408736	27411	408736	
13	20	20962	530550	10481	265275	
14	20	110814	736939	55407	368469.5	
15	20	71918	549787	35959	274893	
16	10	32147	386353	32147	386353	
17	10	26585	346775	26585	346775	

Table 2 : Values of Actual Iron Area

Sample No. (1)	Iron area (2)	Iron Back ground (3)	Actual Iron area (2)-(3) = (4)
1	12255	3779	8776
2	21106	2872	18234
3	17815	3302	14513
4	33529	4141	29388
5	14813.5	4450	10363
6	26918	3551	23367
7	9259	3032	6227
8	17155	4677	12478
9 Fresh Ball	3455	0	3455
10	19170	3290	15880
11	23445	3041	20404
12	27411	4196	23215
13	10481	2723	7758
14	55407	3783	51624
15	35959	2822	33137
16	32147	3966	28180
17	26585	3560	23025

Table 3 : Values of λ

Sample No.	$\lambda = \frac{\text{Area of Iron Transferred}}{\text{Area of Tungston}} = \frac{AFe}{Aw}$
1	$0.023480 = 2.3480 \times 10^{-2}$
2	$0.065174 = 6.5174 \times 10^{-2}$
3	$0.025113 = 2.5113 \times 10^{-2}$
4	$0.072851 = 7.2851 \times 10^{-2}$
5	$0.023910 = 2.3910 \times 10^{-2}$
6	$0.067542 = 6.7542 \times 10^{-2}$
7	$0.021078 = 2.1078 \times 10^{-2}$
8	$0.027392 = 2.7392 \times 10^{-2}$
9	Fresh Ball
10	$0.049548 = 4.9548 \times 10^{-2}$
11	$0.068883 = 6.8883 \times 10^{-2}$
12	$0.0575 = 5.75 \times 10^{-2}$
13	$0.024245 = 2.4245 \times 10^{-2}$
14	$0.140103 = 14.0103 \times 10^{-2}$
15	$0.120545 = 12.0545 \times 10^{-2}$
16	$0.072938 = 7.2938 \times 10^{-2}$
17	$0.066397 = 6.6397 \times 10^{-2}$

Table 4 : Values of λ at different Speeds and Magnetic Fields

Current ampere \ Speed	63 RPM (43.52 m/min) λ	80 RPM (55.25 m/min) λ	100 RPM (69.0 m/min) λ	125 RPM (87.35 m/min) λ
0 Without field	2.3910×10^{-2}	2.5113×10^{-2}	2.384×10^{-2}	2.1078×10^{-2}
4 amp	5.75×10^{-2}	6.8883×10^{-2}	4.9548×10^{-2}	2.4245×10^{-2}
6 amp	6.7542×10^{-2}	7.2851×10^{-2}	6.5174×10^{-2}	2.7392×10^{-2}
8 amp	7.2938×10^{-2}	12.054×10^{-2}	14.01×10^{-2}	6.6397×10^{-2}

where

Current	63 RPM	80 RPM	100 RPM	125 RPM
Without Field	Sample (5)	(3)	(1)	(7)
4 amp	(12)	(11)	(10)	(13)
6 amp	(6)	(4)	(2)	(8)
8 amp	(16)	(15)	(14)	(17)

Sample (9) - Fresh Ball

Table 5 : Values of G at different speeds and magnetic fields

Speed / Current ampere	63 RPM (43.52 m/min) G	80 RPM (55.25 m/min) G	100 RPM (69.0 m/min) G	125 RPM (87.35 m/min) G
4amp	2.4098	2.7410	2.0783	1.3874
6amp	2.8248	2.9009	2.7338	1.2995
8amp	3.0505	4.8021	5.8768	3.1500

Table 6 : R_a value at different cutting speeds and magnetic fields

Current Amperes	R_a at 63 RPM (4352 m/min)	R_a at 80 RPM (55.25 m/min)	R_a at 100 RPM (69 m/min)	R_a at 125 RPM (87.35 m/min)
Without Field	0.5 Min^m	0.28 Min^m	0.25 Min^m	0.22 Min^m
	0.6 Max^m	0.35 Max^m	0.30 Max^m	0.23 Max^m
4	0.70 Min^m	0.55 Min^m	0.37 Min^m	0.30 Min^m
	0.72 Max^m	0.63 Max^m	0.45 Max^m	0.36 Max^m
6	0.85 Min^m	0.70 Min^m	0.45 Min^m	0.38 Min^m
	0.90 Max^m	0.74 Max^m	0.50 Max^m	0.45 Max^m
8	0.98 Min^m	0.80 Min^m	0.49 Min^m	0.45 Min^m
	1.10 Max^m	0.90 Max^m	0.50 Max^m	0.50 Max^m

REFERENCES

1. Sasada T. et al., "The Wear and Mutual Transfer in Copper Ferrous Rubbing", Proc. Fifteenth Japan Congress on Material Research, (1972) pp-1.

2. Ghosh A, "Mechanism of Cutting Tool Wear", Ph.D.Thesis, Calcutta University, (1968).

3. Galie M.T., "Increasing Tool Life by Magnetization", Machines and Cooling, 5 (1973), pp-14.

4. Muju M.K. and Ghosh A, "A Model of Adhesive Wear in Presence of Magnetic Field", Wear, 41 (1977), pp-103.

5. Muju M.K. and Ghosh A, "Effect of Magnetic Field on Wear", Paper presented at the Joint ASME/ASLE Conference, Florida, Oct. 1975.

6. Muju M.K., "Effect of Magnetic Field on Wear", Ph.D.Thesis, I.I.T. Kanpur, 1975.

7. Simpson F.F. and Russel R.W., "Influence of Magnetic Field and the Passage of Electrical Currents on the Deterioration of Ball-bearings", Proc. Conf. Lab. and Wear, (1957), pp-477.

8. D.S. Kamenetskaya, I.B. Piletskaya and Y.I.Schiryayev, Dokl. Akad. Nauk SSSR, 199 (1971), 1289.

9. I.K. Bhat, A.Ghosh, and Muju M.K., "Effect of Magnetic Field on Fatigue", J. of Machine Design, Oct. 1984, Vol.2, pp-59-65.

10. Hirano K, Cohen M, Averback B.L. and Ujiive N, "Self Diffusion in Alpha Iron During Compressive Plastic Flow", Trans. AIME, Vol.227, 1963, p-950.

11. Bullufi R.W. and Ruoff A.L., "On Strain Enhanced Diffusion in Metals-I Point Defects", J. Appl. Phys., Vol.34, 1963, p-1634.

12. Ruoff A.L. and Ballufi, R.W., "Strain Enhanced Diffusion in Metals-II, Dislocations and Grain Boundary Short Circuiting Model", J. Appl. Phys., Vol.34, 1963, p-1848.

13. Brown,A.F. and Blackburn D.A., "Apparent Enhancement of Diffusion Coefficients in Plastically Deformed Metals", Acta. Met. Vol.11, 1963, p-1017.

14. Hart E.W., "On the Role of Dislocation on Bulk Diffusion", Acta Met., Vol.5, 1957, p-597.

15. Muju M.K., "Diffusivity and Diffusion Wear at Higher Strain Rates in Presence of Magnetic Field" - Paper accepted for presentation (and publication) at International Conference on High Productivity Machining, 1985, New Orleans, U.S.A..

16. Radhakrishna A, Muju M.K., Ghosh, A., "Effect of Magnetic Field on Strain Enhanced Wear of Rubbing Surfaces". 9th All India Machine Tool Design and Research Conference (Dec. 10-13, 1984).

17. Srivastava A.K., "Wheel Loading in Fine Grinding", Ph.D. Thesis, I.I.T. Kanpur, 1984.

18. Koing W. and Lortz W., "Three Dimensional Measurement of the Grinding Wheel Surface Evaluation and Effect on Cutting Behaviours", Annals CIRP, Vol.25, 1976, p-197.

19. Shaw M.C., Surface Melting in Grinding Operations", Annals of CIRP, Vol.33, 1984, p-221.

20. T.B. Johansson, R. Akselsson and S.A.E.Johansson, Nucl. Inst. and Meth. 84 (1970), p-141.

21. Ainbinder S. Dzintar R and Klokova E., "Zh.Unit", Izv. AN Latv. SSR 6, 87-98 (1955).

22 Arshinov V.A. and Alekseev G.A., "Meta Cutting Mashgiz" (1953).

23 V.D.Kuznetsov, "Metal Transfer and Build-up in Friction and Cutting", Pergamon Press.

24. Molanin K.I. "Investigation of Material Transfer and Build-up", Thesis Tomsk SFII (1954).

25. Raghuram V., "A Study of the Application of Magnetic Field in Hot Machining", M.Tech. Thesis, 1978, I.I.T. Kanpur.

APPENDIX I

The Statistical Counting Error Involved in PIXE Measurement is as (For Sample No.17)

Channel No (For Iron Peak)	Counts N_{c_i}	$\sqrt{N_{c_i}}$
168	147	12.124
169	152	12.328
170	206	14.352
171	367	19.157
172	692	26.305
173	1199	34.626
174	1914	43.749
175	2877	53.637
176	3661	60.506
177	4154	64.451
178	4036	63.529
179	3466	58.872
180	2597	50.960
181	1698	41.206
182	1069	32.695
183	645	25.396
184	488	22.090
	$\Sigma N_{c_i} = 29313$	$\Sigma \sqrt{N_{c_i}} = 636$

Therefore Actual Counts = 29313 ± 636

and % Error = $\frac{636}{29313} \times 100 = 2.17\%$.

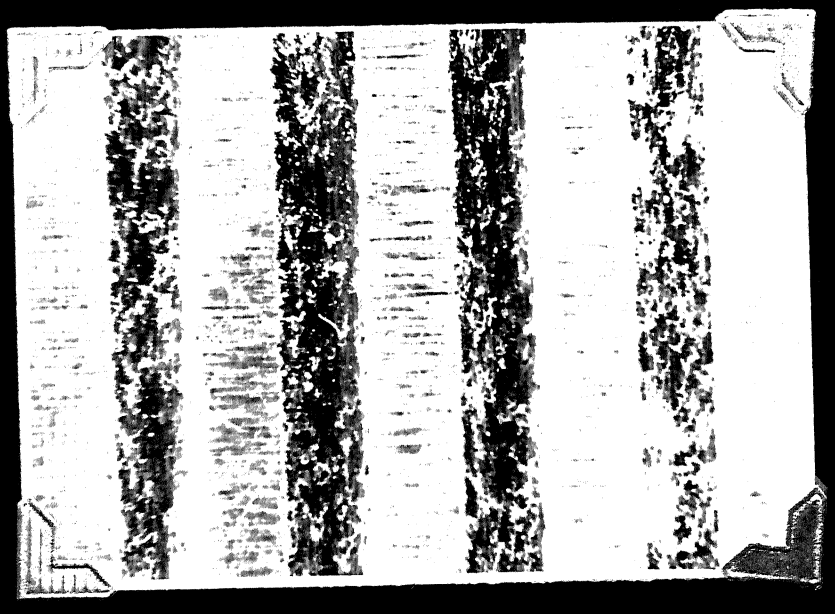

Close-up View of Grooves cut on
Mild Steel Block

Close-up view of adhered iron
on tunguston carbide ball